



This is a repository copy of *Coherence in single photon emission from droplet epitaxy and Stranski–Krastanov quantum dots in the telecom C-band*.

White Rose Research Online URL for this paper:
<http://eprints.whiterose.ac.uk/169947/>

Version: Accepted Version

Article:

Anderson, M., Müller, T., Skiba-Szymanska, J. et al. (6 more authors) (2021) Coherence in single photon emission from droplet epitaxy and Stranski–Krastanov quantum dots in the telecom C-band. *Applied Physics Letters*, 118 (1). 014003. ISSN 0003-6951

<https://doi.org/10.1063/5.0032128>

This article may be downloaded for personal use only. Any other use requires prior permission of the author(s) and AIP Publishing. This article appeared in *Appl. Phys. Lett.* 118, 014003 (2021) and may be found at <https://doi.org/10.1063/5.0032128>.

Reuse

Items deposited in White Rose Research Online are protected by copyright, with all rights reserved unless indicated otherwise. They may be downloaded and/or printed for private study, or other acts as permitted by national copyright laws. The publisher or other rights holders may allow further reproduction and re-use of the full text version. This is indicated by the licence information on the White Rose Research Online record for the item.

Takedown

If you consider content in White Rose Research Online to be in breach of UK law, please notify us by emailing eprints@whiterose.ac.uk including the URL of the record and the reason for the withdrawal request.



eprints@whiterose.ac.uk
<https://eprints.whiterose.ac.uk/>

This is the author's peer reviewed, accepted manuscript. However, the online version of record will be different from this version once it has been copyedited and typeset.

PLEASE CITE THIS ARTICLE AS DOI: 10.1063/5.0032128

Coherence of SK vs DE quantum dots

Coherence in single photon emission from droplet epitaxy and Stranski-Krastanow quantum dots in the telecom C-band

M. Anderson,^{1,2} T. Müller,^{1, a)} J. Skiba-Szymanska,¹ A.B. Krysa,³ J. Huwer,¹ R.M. Stevenson,¹ J. Heffernan,⁴ D.A. Ritchie,² and A.J. Shields¹

¹⁾*Toshiba Europe Limited, Cambridge Research Laboratory, 208 Science Park, Milton Road, Cambridge, CB4 0GZ, UK*

²⁾*Cavendish Laboratory, University of Cambridge, JJ Thomson Avenue, Cambridge, CB3 0HE, UK*

³⁾*EPSRC National Epitaxy Facility, Department of Electronic and Electrical Engineering, University of Sheffield, Mappin Street, Sheffield, S1 3JD, UK*

⁴⁾*Department of Electronic and Electrical Engineering, University of Sheffield, mappin street Sheffield, S1 3JD, UK*

(Dated: 18 December 2020)

This is the author's peer reviewed, accepted manuscript. However, the online version of record will be different from this version once it has been copyedited and typeset.

PLEASE CITE THIS ARTICLE AS DOI: 10.1063/1.50032128

Coherence of SK vs DE quantum dots

The ability of two photons to interfere lies at the heart of many photonic quantum networking concepts, and requires that the photons are indistinguishable with sufficient coherence times to resolve the interference signals. However, for solid-state quantum light sources, this can be challenging to achieve as they are in constant interaction with noise sources in their environment. Here, we investigate the noise sources which affect InAs/InP quantum dots emitting in the telecom C-band, by comparing their behavior on a wetting layer for Stranski-Krastanow grown quantum dots with a nearly wetting layer free environment achieved with the droplet epitaxy growth mode. We show that the droplet epitaxy growth mode is beneficial for a quiet environment, leading to 96% of exciton transitions having a coherence time longer than the typical detector resolution of 100 ps, even under non-resonant excitation. We also show that the decay profile indicates the presence of slow dephasing processes, which can be compensated for experimentally. We finally conduct Hong-Ou-Mandel interference measurements between subsequently emitted photons and find a corrected two-photon interference visibility of 98.6 ± 1.6 % for droplet-epitaxy grown quantum dots. The understanding of the influence of their surroundings on the quantum optical properties of these emitters is important for their optimisation and use in future quantum networking applications.

^{a)}Electronic mail: tina.muller@crl.toshiba.co.uk

This is the author's peer reviewed, accepted manuscript. However, the online version of record will be different from this version once it has been copyedited and typeset.

PLEASE CITE THIS ARTICLE AS DOI: 10.1063/1.50032128

Coherence of SK vs DE quantum dots

Optical quantum networks^{1,2} have many applications ranging from quantum communications³ to distributed quantum computation⁴ and quantum metrology⁵. At the heart of many of its components is the ability of individual photonic qubits to interact via interference. For their development, sources of highly coherent, indistinguishable photons are therefore crucial. To enable efficient long-distance fiber quantum networks, the wavelength of those photons should further be in the telecom C-band, where attenuation can be as little as 0.12 dB/km. This last requirement is particularly challenging given that the most successful quantum light emitters to-date, such as standard quantum dots (QDs) or defects in wide-bandgap semiconductors, emit in the visible or near-infrared part of the spectrum⁶. While photons from these well-understood and developed solid-state emitters have been frequency-converted to the telecom C-band with success^{7,8}, these approaches add experimental complexity as well as suffering from finite conversion efficiency.

As an alternative, quantum light sources directly emitting in the telecom C-band have recently been developed. Most promisingly, these are InAs QDs relying on either strain-relaxing techniques in GaAs-based host materials⁹, or using InP substrates with a smaller lattice mismatch with respect to the QD material¹⁰. Both approaches can provide single and entangled photons¹¹⁻¹⁵, however they differ in the coherence of emission, where the InP material system has proven superior so far^{16,17} and photons with coherence times up to 0.3 of the Fourier limit have been observed¹⁷ even under non-resonant excitation. Long coherence times leading to highly indistinguishable photons are crucial for the efficient quantum communications protocols used in quantum networks, and it is important to understand the sources of noise limiting the performance of the QDs.

Narrow linewidth emission from QDs requires carefully engineered environments using high-quality materials to mitigate sources of noise, and push coherence close to the Fourier limit, where its coherence properties are solely determined by the transition lifetime¹⁸⁻²¹. The main sources of line broadening in QDs are charge noise influencing QD emission frequency via the DC Stark shift²², spin noise affecting the coherence of QD spin states via hyperfine interaction²², and coupling to the phonon bath resulting in a phonon side-band²³ as well as a temperature-dependent broadening of the zero phonon line.

The sensitivity of the QDs to their environment can allow us to learn about the prevalent noise sources affecting them. Here, we compare QDs grown using the droplet epitaxy growth (DE) mode, where the QDs are formed by crystallizing In droplets in an As atmosphere, to InAs/InP QDs grown in the commonly used Stranski-Krastanow (SK) growth mode. The samples investigated here are structurally identical to our earlier work¹⁵, and the growth process for both modes

Coherence of SK vs DE quantum dots

has been described in detail in a previous publication¹². The process is identical for both samples apart from the mode of QD growth, thus we expect differences in the QD noise environment to arise solely from the differences in QD structure resulting from the two growth modes. The samples are grown on (001) oriented substrates by metalorganic vapor phase epitaxy (MOVPE), and the QDs were embedded in a 2λ -cavity with a strongly reflective Bragg mirror below the QDs and a weakly reflecting one above them, to help directing emission towards our collection setup. The innermost three mirror pairs were n-doped for the bottom mirror, and p-doped for the top one, to allow for electrical injection and application of bias voltages. This capability was however not used in the current study. For both samples, QD growth conditions have been optimized to achieve low QD densities $< 10^9/\text{cm}^2$. No further optimization steps for other parameters have been performed in either case.

In contrast to SK QDs, DE QDs show only a minimal residual 2D layer of QD material (wetting layer), which leads to a reduced charge bath felt by each QD. In addition, DE QD formation also does not rely on strain induced by the different crystalline lattice parameters of the QD and the surrounding matrix materials, resulting in an altered strain environment compared to SK QDs. Strain can affect the coupling to phonons and as well as the affinity of the QD to trap charges, which are both potential sources of noise. In our samples, the DE QDs are also slightly smaller in size¹², again altering phonon coupling. To assess the impact of these differences, we collect statistics on coherence times from both types of QDs and compare the absolute values as well as the decay profiles observed in both. We further use DE QDs with long coherence times to show that these enable good mutual indistinguishability values between subsequently emitted photons even under non-resonant excitation.

We start by characterizing the emission from the two types of QDs. For these measurements, the sample is situated in a cryogenic environment at 10 K, and are excited by a continuous wave laser at 780 nm except where explicitly stated otherwise. Light is collected using a fiber-coupled confocal microscope and sent to a spectrometer or superconducting single photon detectors (SSPDs) for analysis.

Both types of QDs show spectra consisting of several sharp lines, as shown in Fig. 1 (a) for DE, and Fig. 1 (b) for SK QDs. From power dependent and fine structure splitting (FSS) measurements, we can identify the neutral exciton (X) in both cases. For DE type QDs, we can further unambiguously identify the biexciton (XX) transition from FSS measurements, and speculate

Coherence of SK vs DE quantum dots

from the doping parameters of our sample¹⁵ that the strongest line is the negatively charged exciton (CX). This spectral signature is typical of DE QDs in this sample and often encountered. In contrast, the spectral profile of SK QDs differs from QD to QD, indicating a rich variety of charge configurations present. As a consequence, it is more difficult to assign specific charge combinations other than X to individual transitions, and we label unidentified transitions X*.

When exciting these transitions using an 80-MHz repetition rate pulsed 780-nm laser and spectrally filtering them before measurement, we can determine their radiative lifetime T_1 , as shown in Fig. 1 (c) and (d). For DE QDs, the XX is fitted to a biexponential decay, where the shorter time constant of 347 ± 2 ps corresponds to the XX lifetime. For the X and CX, single exponentials were used, with fitted time constants of 2.06 ± 0.003 ns and 1.94 ± 0.004 ns, respectively. The fitting region was carefully selected to exclude the initial soft curve due to filling effects especially for the X transition. These filling effects were even more pronounced when looking at the SK lifetimes in 1 (d) and are due to multiexciton relaxation cascades taking place in the QD before the final charge combination is reached^{24–26}. Lifetime measurements were repeated for ten different QDs for both types, with the lifetime statistics summarized in Table I. We note that this measured lifetime likely comprises contributions from both radiative and non-radiative decay channels, where determination of their respective decay rates is left for future studies. The lifetimes for both

	DE QDs		SK QDs	
	mean	s. d.	mean	s. d.
T_1^X (ns)	2.00	0.26	1.63	0.3
T_1^{XX} (ns)	0.33	0.05	0.58	
T_1^{CX} (ns)	1.61	0.24		
$T_1^{X^*}$ (ns)			1.61	0.48

TABLE I. Comparison of lifetime statistics measured for DE and SK QDs. Only one XX transition could be identified in the case of SK QDs.

types of QDs are slower than typically expected for InAs/GaAs QDs emitting around 900 nm. While the size of InAs/InP QDs is similar to their GaAs based counterparts¹², the electron and hole wavefunctions take different forms due to the different host materials²⁷, affecting the exciton

This is the author's peer reviewed, accepted manuscript. However, the online version of record will be different from this version once it has been copyedited and typeset.

PLEASE CITE THIS ARTICLE AS DOI: 10.1063/1.50032128

Coherence of SK vs DE quantum dots

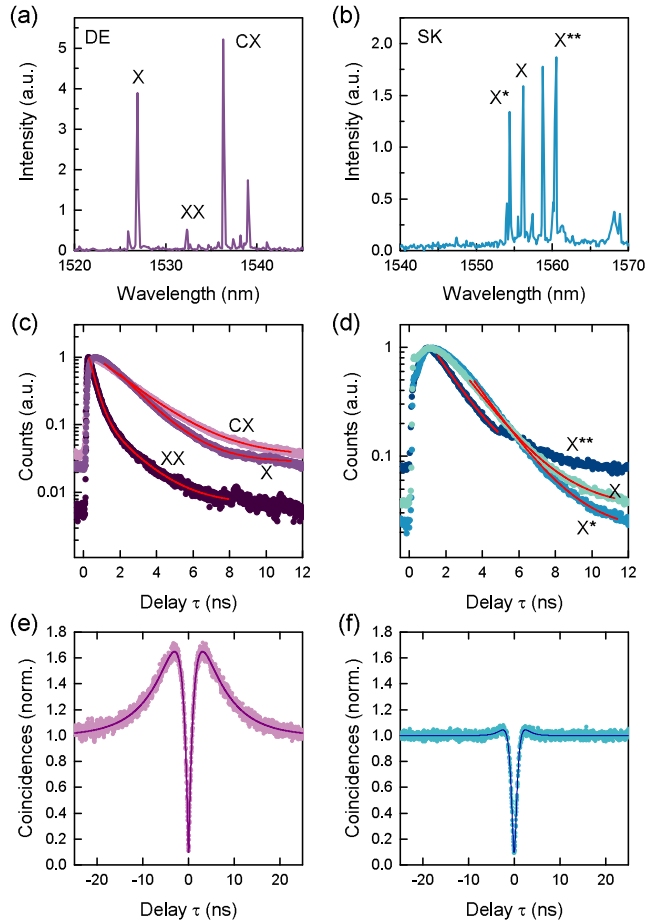


FIG. 1. Spectroscopy of DE vs SK grown quantum dots. (a) and (b) show spectra for the respective cases, (c) and (d) show their select lifetimes as labeled, and (e) and (f) show second order autocorrelations measured for DE and SK QDs, respectively.

recombination times.

We also performed autocorrelation measurements on individual transitions, as shown in Fig. 1 (e) and (f) for DE and SK QDs, respectively. Here, the correlation normalisation is to the time averaged photon pair intensity approximated from the correlation intensity measured far from zero time delay. For DE, the $g^{(2)}(0)$ value is extracted from a fit to a 3-level model and deconvolved

Coherence of SK vs DE quantum dots

from our detector response (100 ps), which yields a value of 0.037 ± 0.004 . The third 'storage' level is the origin of the bunching effect²⁸ observed in this autocorrelation measurement. This bunching is expected to disappear when exciting the system resonantly, as the third level will remain unoccupied in this case. For SK QDs, a fit to a multilevel model was used²⁹. Including deconvolution, the fit gives $g^{(2)}(0) = 0.088 \pm 0.006$. These measurements show that both growth schemes can produce single photon sources in the telecom C-band.

Next, we investigate the coherence time statistics of the two types of QDs. The photon coherence time T_2 depends on the transition lifetime T_1 and the pure dephasing time T_2^* via the relation

$$\frac{1}{T_2} = \frac{1}{2T_1} + \frac{1}{T_2^*}. \quad (1)$$

From Eq. 1, it immediately becomes clear that in the limit of no dephasing, where T_2 is limited only by the lifetime T_1 , its maximum can reach $T_2 = 2T_1$, which is called the Fourier limit.

To allow accurate comparison, all measurements have been taken at the individual QD X saturation power, defined by the power of maximum brightness for the X transition, even if coherence times are expected to be higher at low excitation powers^{17,30}. Using a fiber-based Michelson interferometer (MI) as shown schematically in Fig. 2, we measured the coherence times of 75 DE QD transitions as well as 26 SK QD transitions. For all measurements, T_2 is taken as the time delay after which the visibility of recorded interference fringes has decayed to $1/e$. These measurements take into account both homogenous and inhomogeneous broadening mechanisms. A discussion of their relative contributions to the overall coherence time is given further below. Averaging over all transitions in both cases, the mean coherence time of photons originating from DE QD is 157 ps (standard deviation 72 ps), three times larger than that of photons from SK QD at 51 ps (s. d. 29 ps). The distribution of these coherence times is shown in Fig. 2 (b). Further, the average coherence times for the different transitions in each QD is given in Tab. II.

While the absolute values of T_2 are relevant in practice to resolve interference measurements with finite detector resolution, their ratio to the Fourier limit $2T_1$ measures the intrinsic limitations of the transitions due to dephasing processes. Taking the average lifetimes listed in Tab. I, we calculate the average $T_2/2T_1$ values for transitions from SK vs DE QDs, which are listed in Tab. II and shown in Fig. 2 (c). For X and CX transitions, both types of QDs give low values less than 0.1, however, photons from DE QDs are a factor 1.65 and 1.74 closer to the Fourier limit, respectively. Dephasing rates in SK QDs are therefore stronger compared to their inverse lifetime

This is the author's peer reviewed, accepted manuscript. However, the online version of record will be different from this version once it has been copyedited and typeset.

PLEASE CITE THIS ARTICLE AS DOI: 10.1063/1.50032128

Coherence of SK vs DE quantum dots

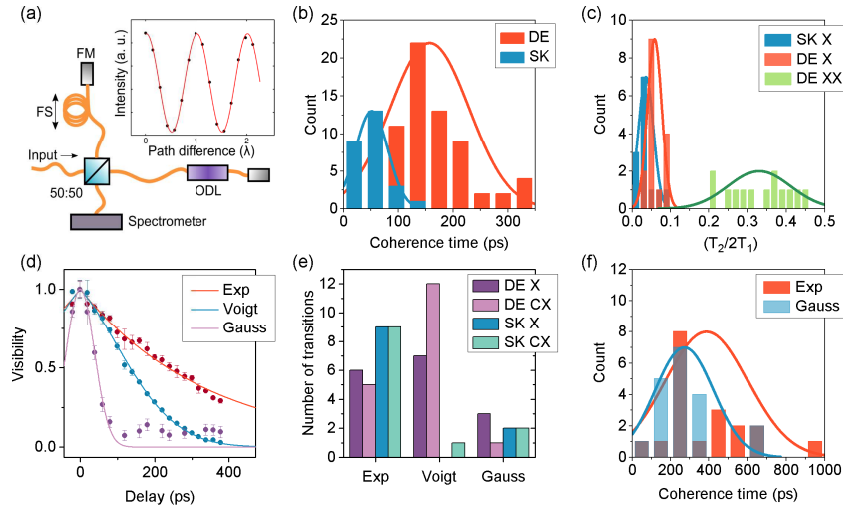


FIG. 2. Coherence time statistics on DE vs SK QDs. (a) Sketch of the fiber-based Michelson interferometer used for coherence time measurements. A 50:50 beam splitter is used to direct the photons to two fibre arms, where they reflected by Faraday mirrors (FMs), and recombined at the same beam splitter before being sent to a spectrometer for detection. One of the arms contains a fibre stretcher (FS) to acquire visibility data (shown in the inset), whereas the other one contains an optical delay line (ODL) to vary the delay between the arm on longer timescales. (b) Histogram of the coherence times of all transitions measured for SK (blue) and DE (red) QDs. Areas where histograms overlap are given in a darker shade in all panels. (c) $T_2/2T_1$ for X transitions in SK and DE QDs, and XX transitions in DE QDs. (d) Example measurements of an exponential, Voigt and Gauss shaped decay of visibility. (e) Line profiles for DE and SK X and CX transitions. (f) Exponential vs Gaussian components in DE X transitions.

than in DE QDs. Remarkably, the average value for DE XX transitions is 0.33, despite the QD being driven at saturation power. The reason for this high value is the short XX lifetime, whereas the pure dephasing rate T_2^* is not diminished.

Dephasing processes can be distinguished by their timescale compared to the transition lifetime³¹. Fast dephasing processes originating from phonon coupling or coupling to the electronic noise from a charge bath will result in a Lorentzian spectrum in the frequency domain and an exponential decay of coherence over time, whereas slow processes driven for example by fluctuating

This is the author's peer reviewed, accepted manuscript. However, the online version of record will be different from this version once it has been copyedited and typeset.

PLEASE CITE THIS ARTICLE AS DOI: 10.1063/1.50032128

Coherence of SK vs DE quantum dots

	DE QDs		SK QDs	
	mean	s. d.	mean	s. d.
T_2 all lines	157	72	51	29
T_2^X	230.1	74.6	58	32
T_2^{XX}	105	31		
T_2^{CX}	240	124		
$T_2^{X^*}$			45	27
$T_2^X/2T_1^X$	0.056	0.019	0.035	0.002
$T_2^{XX}/2T_1^{XX}$	0.33	0.08		
$T_2^{CX}/2T_1^{CX}$	0.047	0.022		
$T_2^{X^*}/2T_1^{X^*}$			0.027	0.017

TABLE II. Comparison of coherence time statistics measured for DE and SK quantum dots. T_2 values are given in ps.

individual charges in the environment result in a Gaussian spectrum in the frequency domain and Gaussian decay of coherence over time. If both types of dephasing are present, a Voigt profile is observed. This profile is described in the frequency domain by the convolution of the Gaussian and Lorentzian component, which results in the simple multiplication of the Gaussian and exponential components in the time domain. The observed decay profile therefore gives some insight into the underlying physical mechanisms responsible for the dephasing.

In our measurements, all three decay profiles are observed, and Fig. 2 (d) shows examples of Gaussian, Voigt and exponential profiles seen from different QDs. Comparing the profiles observed from the X and CX/X* transitions of DE and SK QDs, it is striking that the majority of SK QDs (18 out of 23 cases) exhibit an exponential decay in coherence, whereas the majority of DE QDs (24 out of 34 cases) show a Gaussian contribution as well. This is shown graphically in Fig. 2 (e). This is a strong indication that the dephasing mechanisms limiting the photons' spectral width in SK QDs are fast processes. The average inverse Lorentzian dephasing rate for SK QDs is 56.1 ± 26.8 ps. In contrast, looking at DE X and CX transitions and comparing the

Coherence of SK vs DE quantum dots

inverse dephasing rates of the Gaussian vs Lorentzian contributions to their dephasing, we find that the the mean Lorentzian contribution results in inverse dephasing rates of 271 ps (s. d. 153 ps), indicating that fast dephasing processes are about 5 times weaker here. This allows for the resolution of a Gaussian contribution with a mean inverse dephasing rate of 387 ps (s. d. 215 ps) as well. Statistics on the Gaussian and Exponential contributions to inverse dephasing are shown in Fig. 2 (f). In both types of QDs, there are also a few QDs affected by very strong pure Gaussian dephasing, which is consistent with charges trapped in the vicinity of the QDs, for example at impurity sites³². This indicates a similar quality of host material for both types of QDs, as expected from their similar growth protocol.

To elucidate the mechanisms responsible for the dephasing in these QDs, we combine their coherence statistics with a comparison of their physical differences. Given that the QDs in both growth modes are formed of the same species, with the SK QDs being slightly bigger, we would expect spin noise to be more pronounced in DE QDs, as it depends on the number of spins as $1/\sqrt{N}$ with N the number of spins²². We therefore consider spin noise unlikely to be the dominant dephasing mechanism in these QDs. Considering the impact of lattice vibrations, we note that phonon sidebands are largely filtered out in our interferometer setup (bandwidth ~ 0.5 nm), and we are left with the pure broadening of the zero-phonon line. Compared to the effects of spin and charge noise, the broadening induced by lattice vibrations is generally found to be weak at low temperatures^{18,23,33}, and is also not expected to increase in coupling strength under non-resonant excitation. We therefore speculate that it is charge noise which mainly limits coherence in the samples, both for SK and DE QDs. This is widely seen in the literature under non-resonant excitation^{18,22,33}. While it is unusual to observe charge noise at the fast timescales seen here and is typically associated with inhomogeneous broadening leading to Gaussian lineshapes³³, we can speculate that the relatively long radiative lifetimes in these QDs may contribute to the manifestation of charge noise in Lorentzian or Voigt profiles. We conclude that the smaller wetting layer, potentially in conjunction with the altered strain in DE QDs, leads to a reduced charge bath, and consequently results in a calmer environment for spins in DE QDs, with potential for further improvement when using resonant excitation techniques.

Next, we investigate the indistinguishability of photons from the telecom-wavelength QDs. Given our detector resolution of 100 ps, we expect good interference visibility from transitions with coherence times above this value. From Tab. II, we calculate that this is the case for 95% of DE X and 79% of all DE QD transitions, but only for 9% of SK X and 5% of all transitions

Coherence of SK vs DE quantum dots

from S-K QDs. We therefore limit our study to DE QDs and focus on an X transition for which a coherence time of 443 ± 23 ps was measured using the MI. Here, the QD was excited with 1310-nm light, and the intensity was set at five times below saturation.

Indistinguishability of photons is measured using a fiber-based Hong-Ou-Mandel interferometer³⁴, as sketched in Fig. 3 (a), where the delay between the two interferometer arms at 6.25 ns is longer than the natural lifetime of the measured transition. A linear polarizer is used to filter a particular polarisation of photons from the QD, and photons are made distinguishable by rotating the polarisation in one arm by 90 degrees with respect to the other. Here, we consider the QD X transition, which consists of a frequency doublet, where the two spectral components are due to electron-hole pairs with opposite spin orientation being offset in energy by the FSS and are orthogonally polarised. To simulate conditions where the QD functions in a quantum network application and all photons need to be used, we set it to allow 50% of each FSS transition into the interferometer. The spectrum of the impinging light is given by a frequency doublet, and we are able to resolve the resulting beats in the interference pattern.

The X photon pulse in the time domain in our case is given by

$$\xi(t) = \begin{cases} Ae^{-\frac{t}{T_2} - \frac{1}{2}i(\Delta\omega + 2\omega_0)t} (1 + e^{i\Delta\omega}) & t \geq 0 \\ 0 & \text{otherwise,} \end{cases} \quad (2)$$

where A is a normalisation constant, ω_0 is the center frequency of the transition, and $\Delta\omega$ is the energy splitting given by the FSS. This function describes a wave packet with an envelope given by an exponential decay at timescale T_2 and an oscillating part consisting of two frequency components separated by $\Delta\omega$, after emission of a QD photon at time $t = 0$. Using this expression, we can calculate the expected correlations for co-polarized (\parallel , $\phi = 0$) and cross-polarized (\perp , $\phi = \pi/2$) light as follows:

$$g_{\phi}^{(2)}(\tau) = \frac{1}{2}g^{(2)}(\tau) + \frac{1}{2} [g^{(2)}(\tau + \Delta\tau) + g^{(2)}(\tau - \Delta\tau)] P_{HOM}(\tau, \phi). \quad (3)$$

Here, the first term describes the expected correlation between two photons which have traveled through the same arm in the setup, whereas the second term describes the expected correlation between photons which have traveled through opposite arms in the setup. the $g^{(2)}(\tau)$ are taken from independent fits to separately recorded autocorrelation measurements, such as those presented in Fig. 1, $\Delta\tau$ is the delay between photons determined by the interferometer, $P_{HOM}(\tau, \perp) = 0.5$, and $P_{HOM}(\tau, \parallel)$ is determined numerically from Equation 2 by calculating the joint probability of

Coherence of SK vs DE quantum dots

detecting a photon in each output arm for all possible emission and detection times. From these, the visibility V_{HOM} in our setup can be calculated as

$$V_{HOM}(\tau) = 1 - \frac{g_{\parallel}^{(2)}(\tau)}{g_{\perp}^{(2)}(\tau)}. \quad (4)$$

The resulting correlations for co- and cross-polarized photons around zero delay are shown in Fig. 3 (b). The cross-polarized coincidence curve shows a dip below 1, as expected. The optimal value

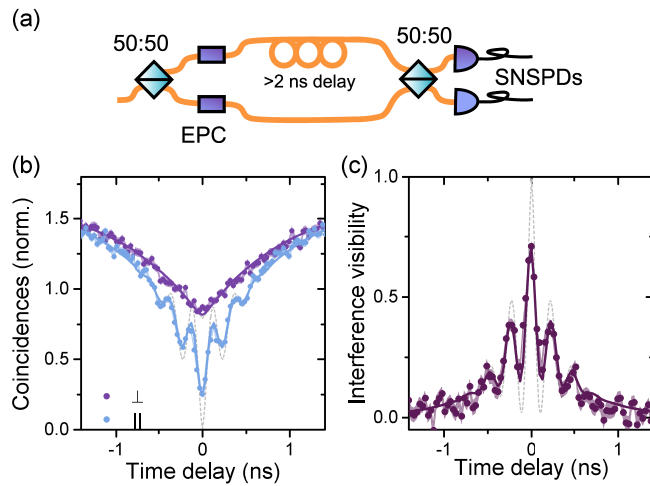


FIG. 3. Indistinguishability of photons from DE quantum dots. (a) Sketch of the fiber-based Hong-Ou-Mandel setup, where the polarisation of photons propagating in the two arms is set by electronic polarisation controllers (EPCs) and superconducting single photon detectors (SNSPDs) are used to measure coincidences. (b) Raw two-photon intensities for distinguishable (purple) and indistinguishable (blue) photons. Circles denote data points, solid lines are fits as described in the text, and shaded areas denote error bars. (c) Visibility calculated from the curves in (b), where again data points are given by circles, the fit by the solid line and error bars by the shaded region.

of 0.5 according to Equation 3 is not reached, however, which is mainly due to bunching effects in the autocorrelation functions. For the co-polarized case, we see the expected oscillations resulting from the double-Lorentzian input spectrum. A fit using our model describes the data perfectly and indicates a FSS of 17 μeV , consistent with an independent spectral measurement for this QD. We

Coherence of SK vs DE quantum dots

can further extract the coherence time under these excitation conditions, which at $T_2 = 440 \pm 45$ ps is consistent with independent measurements in an MI. Here, the detector resolution significantly affects the recorded coincidence curve: deconvolving a fit to the raw two-photon intensities with our detector resolution reveals a dip reaching down to 0.01 ± 0.01 . The resulting interference visibility is shown in Fig. 3 (c). While the raw measured two-photon intensities give a maximum visibility of 71.3 ± 1.6 %, deconvolving the fit to the data with the detector response increases the visibility to 98.6 ± 1.6 . This value compares well with the recently reported indistinguishability measured on GaAs-based C-band quantum QDs, even though those results were achieved under resonant excitation¹⁶. In conclusion, we report a comparison between the coherence properties of SK and DE QDs, where the DE growth mode is shown to provide a superior material system and a calmer environment to the QD spins. This leads to coherence times exceeding the typical detector resolution of 100 ps for 95% of DE X transitions. We found strong indications that the main source of dephasing in both is charge noise, in line with previous findings when exciting GaAs based QDs non-resonantly^{18,33}. This noise is reduced in DE QDs due to their lower strain and much reduced wetting layer, leading to a reduced charge bath in the QD environment. The decay profile for DE QDs further indicates that noise mechanisms are partly due to slow processes, allowing compensation of decoherence using echo-type setups. Future studies could investigate whether a bias voltage applied across our devices can reduce charge fluctuations in the QD environment even further. Lastly we show near-ideal indistinguishability of subsequently emitted photons from DE QDs. While we expect the true limits of photon indistinguishability and coherence to be revealed in resonant excitation experiments^{16,22}, our results indicate that InAs/InP DE QDs provide a promising material platform for telecom wavelength quantum network applications.

ACKNOWLEDGMENTS

The authors acknowledge partial financial support from the Engineering and Physical Sciences Research Council and the UK's innovation agency, Innovate UK. M. A. gratefully acknowledges support from the Industrial CASE award funded by the EPSRC and Toshiba Research Europe Limited.

This is the author's peer reviewed, accepted manuscript. However, the online version of record will be different from this version once it has been copyedited and typeset.

PLEASE CITE THIS ARTICLE AS DOI: 10.1063/1.50032128

Coherence of SK vs DE quantum dots

DATA AVAILABILITY

The data that support the findings of this study are available from the corresponding author upon reasonable request.

REFERENCES

- ¹E. Knill, R. Laflamme, and G. J. Milburn, "A scheme for efficient quantum computation with linear optics," *Nature* **409**, 46–52 (2001).
- ²H. J. Kimble, "The quantum internet," *Nature* **453**, 1023–1030 (2008).
- ³N. Gisin and R. Thew, "Quantum communication," *Nature Photonics* **1**, 165–171 (2007).
- ⁴J. I. Cirac, A. K. Ekert, S. F. Huelga, and C. Macchiavello, "Distributed quantum computation over noisy channels," *Physical Review A* **59**, 4249–4254 (1999).
- ⁵P. Kómár, E. M. Kessler, M. Bishof, L. Jiang, A. S. Sørensen, J. Ye, and M. D. Lukin, "A quantum network of clocks," *Nature Physics* **10**, 582–587 (2014).
- ⁶I. Aharonovich, D. Englund, and M. Toth, "Solid-state single-photon emitters," *Nature Photonics* **10**, 631–641 (2016).
- ⁷J. H. Weber, B. Kambs, J. Kettler, S. Kern, J. Maisch, H. Vural, M. Jetter, S. L. Portalupi, C. Becher, and P. Michler, "Two-photon interference in the telecom C-band after frequency conversion of photons from remote quantum emitters," *Nature Nanotechnology* **14**, 23–26 (2019).
- ⁸A. Tchebotareva, S. L. N. Hermans, P. C. Humphreys, D. Voigt, P. J. Harmsma, L. K. Cheng, A. L. Verlaan, N. Dijkhuizen, W. de Jong, A. Dréau, and R. Hanson, "Entanglement between a diamond spin qubit and a photonic time-bin qubit at telecom wavelength," *Physical Review Letters* **123**, 063601 (2019).
- ⁹S. L. Portalupi, M. Jetter, and P. Michler, "InAs quantum dots grown on metamorphic buffers as non-classical light sources at telecom C-band: a review," *Semiconductor Science and Technology* **34**, 053001 (2019).
- ¹⁰D. Kim, J. Lefebvre, J. Mckee, S. Studenikin, R. L. Williams, A. Sachrajda, P. Zawadzki, P. Hawrylak, W. Sheng, G. C. Aers, and P. J. Poole, "Photoluminescence of single, site-selected, InAsInP quantum dots in high magnetic fields," *Applied Physics Letters* **87**, 212105 (2005).
- ¹¹M. Benyoucef, M. Yacob, J. P. Reithmaier, J. Kettler, and P. Michler, "Telecom-wavelength (1.5 μ m) single-photon emission from inp-based quantum dots," *Applied Physics Letters* **103**,

This is the author's peer reviewed, accepted manuscript. However, the online version of record will be different from this version once it has been copyedited and typeset.

PLEASE CITE THIS ARTICLE AS DOI: 10.1063/5.0032128

Coherence of SK vs DE quantum dots

- 162101 (2013).
- ¹²J. Skiba-Szymanska, R. M. Stevenson, C. Varnava, M. Felle, J. Huwer, T. Müller, A. J. Bennett, J. P. Lee, I. Farrer, A. B. Krysa, P. Spencer, L. E. Goff, D. A. Ritchie, J. Heffernan, and A. J. Shields, “Universal growth scheme for quantum dots with low fine-structure splitting at various emission wavelengths,” *Physical Review Applied* **8** (2017).
- ¹³F. Olbrich, J. Höschele, M. Müller, J. Kettler, S. Luca Portalupi, M. Paul, M. Jetter, and P. Michler, “Polarization-entangled photons from an InGaAs-based quantum dot emitting in the telecom C-band,” *Applied Physics Letters* **111**, 133106 (2017).
- ¹⁴C. Carmesin, F. Olbrich, T. Mehrrens, M. Florian, S. Michael, S. Schreier, C. Nawrath, M. Paul, J. Höschele, B. Gerken, J. Kettler, S. L. Portalupi, M. Jetter, P. Michler, A. Rosenauer, and F. Jahnke, “Structural and optical properties of InAs/(In)GaAs/GaAs quantum dots with single-photon emission in the telecom C-band up to 77 K,” *Physical Review B* **98** (2018).
- ¹⁵T. Müller, J. Skiba-Szymanska, A. B. Krysa, J. Huwer, M. Felle, M. Anderson, R. M. Stevenson, J. Heffernan, D. A. Ritchie, and A. J. Shields, “A quantum light-emitting diode for the standard telecom window around 1,550 nm,” *Nature Communications* **9**, 862 (2018).
- ¹⁶C. Nawrath, F. Olbrich, M. Paul, S. L. Portalupi, M. Jetter, and P. Michler, “Coherence and indistinguishability of highly pure single photons from non-resonantly and resonantly excited telecom C-band quantum dots,” *Applied Physics Letters* **115**, 023103 (2019).
- ¹⁷M. Anderson, T. Müller, J. Huwer, J. Skiba-Szymanska, A. B. Krysa, R. M. Stevenson, J. Heffernan, D. A. Ritchie, and A. J. Shields, “Quantum teleportation using highly coherent emission from telecom C-band quantum dots,” *npj Quantum Information* **6** (2020).
- ¹⁸A. V. Kuhlmann, J. H. Prechtel, J. Houel, A. Ludwig, D. Reuter, A. D. Wieck, and R. J. Warburton, “Transform-limited single photons from a single quantum dot,” *Nature Communications* **6**, 8204 (2015).
- ¹⁹N. Somaschi, V. Giesz, L. de Santis, J. C. Loredó, M. P. Almeida, G. Hornecker, S. L. Portalupi, T. Grange, C. Antón, J. Demory, C. Gómez, I. Sagnes, N. D. Lanzillotti-Kimura, A. Lemaître, A. Auffeves, A. G. White, L. Lanco, and P. Senellart, “Near-optimal single-photon sources in the solid state,” *Nature Photonics* **10**, 340–345 (2016).
- ²⁰H. Wang, Z.-C. Duan, Y.-H. Li, S. Chen, J.-P. Li, Y.-M. He, M.-C. Chen, Y. He, X. Ding, C.-Z. Peng, C. Schneider, M. Kamp, S. Höfling, C.-Y. Lu, and J.-W. Pan, “Near-transform-limited single photons from an efficient solid-state quantum emitter,” *Physical Review Letters* **116**, 213601 (2016).

This is the author's peer reviewed, accepted manuscript. However, the online version of record will be different from this version once it has been copyedited and typeset.

PLEASE CITE THIS ARTICLE AS DOI: 10.1063/1.50032128

Coherence of SK vs DE quantum dots

- ²¹F. Liu, A. J. Brash, J. O'Hara, L. M. P. P. Martins, C. L. Phillips, R. J. Coles, B. Royall, E. Clarke, C. Bentham, N. Prtljaga, I. E. Itskevich, L. R. Wilson, M. S. Skolnick, and A. M. Fox, "High purcell factor generation of indistinguishable on-chip single photons," *Nature Nanotechnology* **13**, 835–840 (2018).
- ²²A. V. Kuhlmann, J. Houel, A. Ludwig, L. Greuter, D. Reuter, A. D. Wieck, M. Poggio, and R. J. Warburton, "Charge noise and spin noise in a semiconductor quantum device," *Nature Physics* **9**, 570–575 (2013).
- ²³J. Iles-Smith, D. P. S. McCutcheon, A. Nazir, and J. Mørk, "Phonon scattering inhibits simultaneous near-unity efficiency and indistinguishability in semiconductor single-photon sources," *Nature Photonics* **11**, 521–526 (2017).
- ²⁴E. Dekel, D. V. Regelman, D. Gershoni, E. Ehrenfreund, W. V. Schoenfeld, and P. M. Petroff, "Cascade evolution and radiative recombination of quantum dot multiexcitons studied by time-resolved spectroscopy," *Physical Review B* **62**, 11038–11045 (2000).
- ²⁵T. Kuroda, S. Sanguinetti, M. Gurioli, K. Watanabe, F. Minami, and N. Koguchi, "Picosecond nonlinear relaxation of photoinjected carriers in a single GaAs/Al_{0.3}Ga_{0.7}As quantum dot," *Physical Review B* **66** (2002).
- ²⁶N. Ha, T. Mano, S. Dubos, T. Kuroda, Y. Sakuma, and K. Sakoda, "Single photon emission from droplet epitaxial quantum dots in the standard telecom window around a wavelength of 1.55 μ m," *Applied Physics Express* **13**, 025002 (2020).
- ²⁷L. He, M. Gong, C.-F. Li, G.-C. Guo, and A. Zunger, "Highly reduced fine-structure splitting in InAs/InP quantum dots offering an efficient on-demand entangled 1.55-microm photon emitter," *Physical Review Letters* **101**, 157405 (2008).
- ²⁸S. C. Tapster, P. Jonsson, J. G. Rarity, and P. R. Tapster, "Intensity fluctuation spectroscopy of small numbers of dye molecules in a microcavity," *Physical Review A* **58**, 620–628 (1998).
- ²⁹G. Sallen, A. Tribu, T. Aichele, R. André, L. Besombes, C. Bougerol, S. Tatarenko, K. Kheng, and J. P. Poizat, "Exciton dynamics of a single quantum dot embedded in a nanowire," *Physical Review B* **80**, 085310 (2009).
- ³⁰A. Berthelot, I. Favero, G. Cassabois, C. Voisin, C. Delalande, P. Roussignol, R. Ferreira, and J. M. Gérard, "Unconventional motional narrowing in the optical spectrum of a semiconductor quantum dot," *Nature Physics* **2**, 759–764 (2006).
- ³¹R. Loudon, *The quantum theory of light*, 3rd ed. (Oxford University Press, Oxford, 2000).

This is the author's peer reviewed, accepted manuscript. However, the online version of record will be different from this version once it has been copyedited and typeset.

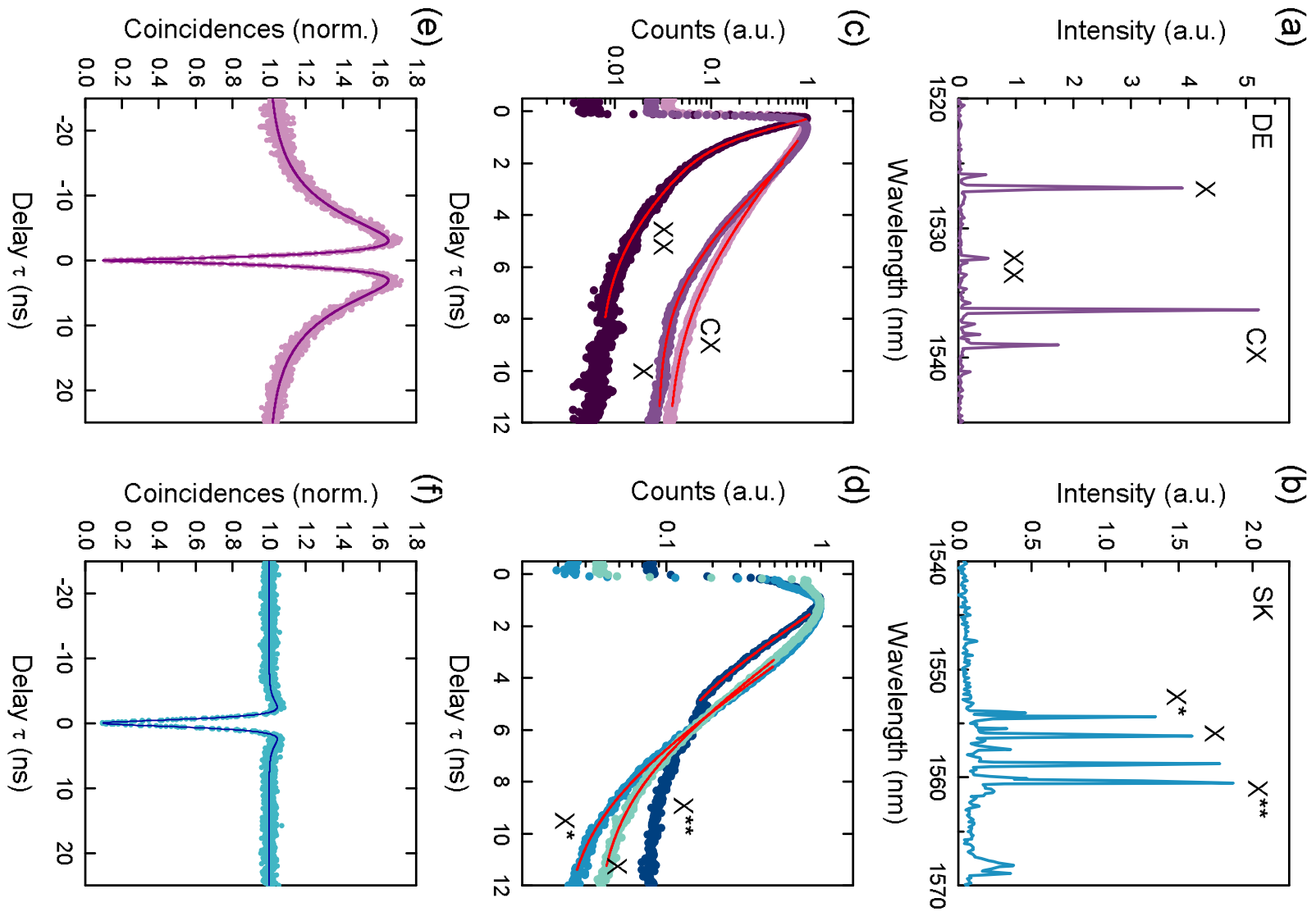
PLEASE CITE THIS ARTICLE AS DOI: 10.1063/5.0032128

Coherence of SK vs DE quantum dots

- ³²H. Kamada and T. Kutsuwa, “Broadening of single quantum dot exciton luminescence spectra due to interaction with randomly fluctuating environmental charges,” *Physical Review B* **78** (2008).
- ³³H. Vural, S. L. Portalupi, and P. Michler, “Perspective of self-assembled InGaAs quantum-dots for multi-source quantum implementations,” *Applied Physics Letters* **117**, 030501 (2020).
- ³⁴Hong, Ou, and Mandel, “Measurement of subpicosecond time intervals between two photons by interference,” *Physical Review Letters* **59**, 2044–2046 (1987).

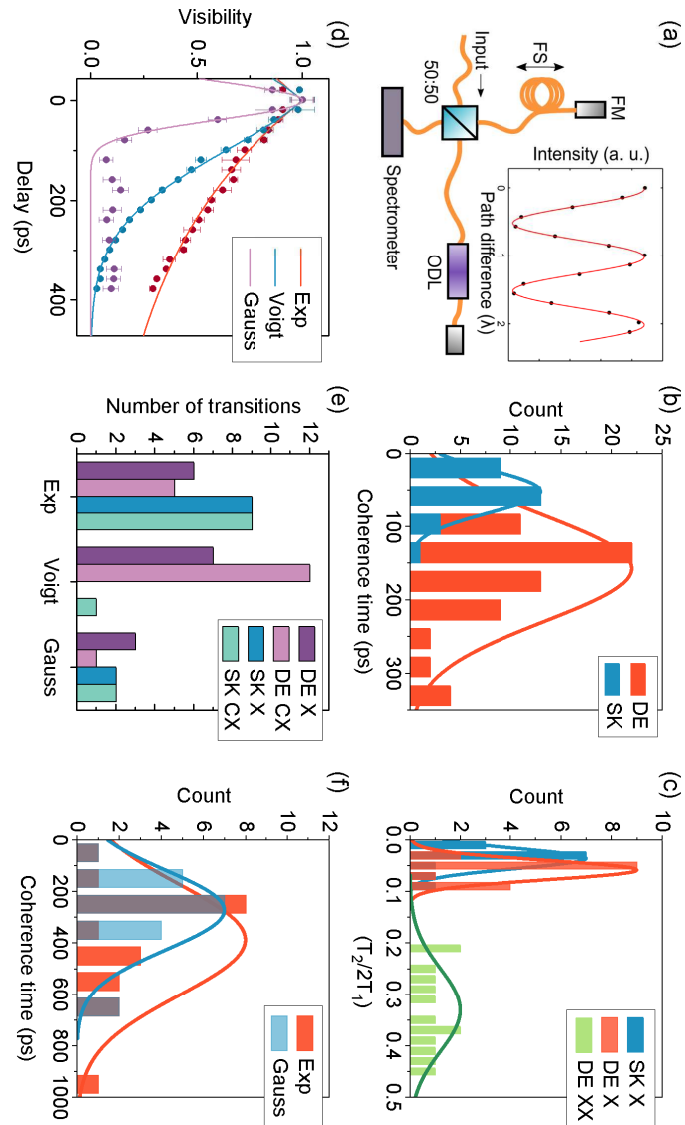
This is the author's peer reviewed, accepted manuscript. However, the online version of record will be different from this version once it has been copyedited and typeset.

PLEASE CITE THIS ARTICLE AS DOI: 10.1063/5.0032128



This is the author's peer reviewed, accepted manuscript. However, the online version of record will be different from this version once it has been copyedited and typeset.

PLEASE CITE THIS ARTICLE AS DOI: 10.1063/5.0032128



This is the author's peer reviewed, accepted manuscript. However, the online version of record will be different from this version once it has been copyedited and typeset.

PLEASE CITE THIS ARTICLE AS DOI: 10.1063/5.0032128

